ELSEVIER

Diamond and Related Materials 12 (2003) 799–805

DIAMOND AND RELATED MATERIALS

www.elsevier.com/locate/diamond

Feasibility studies of magnetic particle-embedded carbon nanotubes for perpendicular recording media

Cheng Tzu Kuo*, Chao Hsun Lin, An Ya Lo

Department of Materials Science and Engineering, National Chiao Tung University, 1001 Ta-Hsueh Road, Hsinchu 300, Taiwan, ROC

Abstract

Nano-sized magnetic particles were successfully used as the catalysts to synthesize magnetic metal-encapsulated carbon nanotubes (CNTs) or nanoparticles on Si wafers in a microwave plasma electron cyclotron resonance chemical vapor deposition (ECR-CVD) system with CH_4 and/or H_2 as source gases. The magnetic catalyst materials, including Fe–Pt, Co–Pt, $Nd_2Fe_{14}B$, Fe and Fe–Ni, were first deposited on Si wafers by a physical vapor deposition (PVD) method, with subsequent plasma treatment for nanoparticle transformation. The main process parameters include catalyst materials, hydrogen plasma catalyst pretreatment and deposition temperature. For applications in magnetic media, the process has the following advantages: perpendicularly aligned CNTs or nanoparticles; tip-growth CNTs; well-distributed magnetic particles; detectable magnetic field in each particle; high tube number density (up to 134 Gtubes/inch^2 for Fe-assisted CNTs); favorable catalyst size; higher shape and induced anisotropy; and nanostructures that can be manipulated. The catalyst particle sizes of Fe, $Nb_2Fe_{14}B$ and Fe–Pt (35–40 nm in diameter) are uniform and greater than but close to the critical optimum size or single domain size, which favor a higher coercive force. The greatest coercive force can reach 750 Oe for Fe-assisted CNTs at a deposition temperature of 715 °C, which is comparable with values reported in the literature. The coercive force difference between the vertical and horizontal directions can reach 300 Oe for Fe-assisted CNTs, and 355 Oe for $Nb_2Fe_{14}B$-assisted CNTs.

Keywords: Carbon nanotubes; Catalyst; Cyclotron resonance CVD; Magnetic recording; Perpendicular recording media

1. Introduction

Higher-areal-density magnetic recording media are being demanded in industries due to their great market volume. The way to increase the density is to minimize the signal spot size. Storage media can be broadly divided into three series, i.e. magnetic, optical and semiconductor storage media. Magnetic storage media include the traditional tapes and videocassettes, hard disks for mainframe computers, floppy disks for personal computers (PC), portable ZIP and MO disks (magneto-optic) with high storage capacity. Their development has covered a wide historical period, ranging from the industrial era to the mainframe and PC eras and up to the post-PC era, or in terms of years from 1970 to 2001. Because of the great market volume and the long development period, magnetic storage media have become an everyday commodity. For storage capacity, a minimum signal spot of <100 nm is required for a terabyte capacity, and of <20 nm for greater than terabyte capacity.

Based on the orientation of the magnetic domains in magnetic storage media, they can be broadly divided into two categories, i.e. the horizontally oriented and vertically oriented types. The results reported indicate that horizontally-oriented magnetic storage media may reach the limit in physics for storage capacity of >40 Gbit/inch^2 [1,2]. In the present commercial hard-disk market, the horizontally oriented type is generally adopted for all magnetic storage media, except MO media, for which the vertically oriented type is used. In order to overcome the bottleneck of the horizontally oriented storage media, changing the recording type, such as vertically oriented or patterned media, is theoretically possible. A few hard disk manufacturers and research institutes have successfully designed such prototype media to demonstrate their feasibility [1,3–9]. However,

*Corresponding author. Tel.: +886-3-5731949; fax: +886-3-5721065.

E-mail address: ctkuo@mail.nctu.edu.tw (C.T. Kuo).

0925-9635/03/$ © 2002 Elsevier Science B.V. All rights reserved.
PII: S0925-9635(02)00231-5

Table 1
Specimen designation, pretreatment and deposition conditions

Specimen designation	Catalyst	Substrate temperature (°C)	Working pressure (10^{-3} torr)	H plasma etching
A1	Fe–Pt	705	6.2	Yes
A2	Fe–Pt	673	5.5	No
B1	Co–Pt	715	6.3	Yes
B2	Co–Pt	673	5.5	No
C1	$Nd_2Fe_{14}B$	717	6.4	Yes
C2	$Nd_2Fe_{14}B$	590	6.2	Yes
C3	$Nd_2Fe_{14}B$	620	5.8	Yes
C4	$Nd_2Fe_{14}B$	660	6.6	Yes
C5	$Nd_2Fe_{14}B$	685	5.9	Yes
C6	$Nd_2Fe_{14}B$	700	6.5	Yes
D1	Fe	715	6.3	Yes
D2	Fe	673	5.5	No
E1	Fe–Ni	705	6.2	Yes

Other deposition conditions: microwave power, 800 W; magnetic field, 875 G; flow ratio, CH_4/H_2 = 15 sccm:15 sccm; and bias, −200 V. H plasma etching conditions: H_2, 15 sccm; bias, −200 V.

many problems must be solved before commercialization, including: (1) design and fabrication techniques for a high-precision recording head and servo driving system; (2) fabrication parameters for storage media, such as size uniformity (dispersion <10%), morphology control, higher magnetic properties (higher coercive field strength H_c, higher squareness ratio S, higher anisotropic magnetic crystal, lower noise, etc.); lower cost, etc.

This work was planned to study the feasibility of nano-resolution magnetic storage media using state-of-the-art nanostructure fabricating techniques. Magnetic nanoparticles on substrates act as the catalysts to synthesize protective layers of carbon nanotubes or nanoparticles on themselves.

2. Experimental

Carbon nanotubes/nanoparticles were synthesized on magnetic metal-coated substrates of p-type silicon wafers by electron cyclotron resonance chemical vapor deposition (ECR-CVD) methods. The catalyst magnetic materials, including Fe, Fe–Pt, Fe–Ni, Co–Pt and $Nb_2Fe_{14}B$, were coated on Si wafers with pure Fe or alloys as targets by PVD. Most of the magnetic metal-coated substrates were pretreated with hydrogen plasma under additional electrical heating to the desired temperature. After hydrogen plasma pretreatment, the specimens immediately underwent CNT deposition. The effects of magnetic catalyst materials, pretreatments and deposition temperature were examined. The specimen designation, catalyst pretreatment and deposition conditions are shown in Table 1. Magnetic field strength of 875 G was applied to maintain the ECR condition. The magnetic properties, morphology, microstructure and bonding structures of the magnetic catalyst-assisted carbon nanostructures were characterized by vibration sample magnetometry (VSM), magnetic force microscopy (MFM), atomic force microscopy (AFM), scanning electron microscopy (SEM), transmission electron microscopy (TEM) and high-resolution transmission electron microscopy (HRTEM).

3. Results and discussion

3.1. Effects of magnetic catalyst material

The morphology features, adhesion and magnetic properties of the magnetic metal-assisted CNTs are shown in Table 2. The corresponding side-view and top-view SEM micrographs for different magnetic catalysts are depicted in Fig. 1 for Fe, Fe–Pt, Co–Pt, $Nb_2Fe_{14}B$ and Fe–Ni catalysts. From the point of view of applications in recording media, all CNTs here take advantage of the vertically aligned and tip-growth CNTs instead of base-growth CNTs. The results show that under the same deposition conditions, different catalysts can produce CNTs with different morphology features and properties, such as differences in tube number density, tube length, carbon film formation, bonding between catalyst and CNTs, growth mechanism and type of

Table 2
Morphology features and properties of the catalyst-assisted CNTs

	Specimen designation				
	A1	B1	C1	D1	E1
Catalyst material	Fe–Pt	Co–Pt	$Nd_2Fe_{14}B$	Fe	Fe–Ni
Tube length (nm)	170	170	2100	1500	600
Tube diameter (nm)	50	60–180	60	60	50–120
Tube number density (Gtubes/inch^2)	77	16	71	134	39
Diameter of catalyst particle (nm)	40	20–120	35	35	10–100
Graphene layer alignment	Poor	–	Good	–	Good
Adhesion	Fair	Fair	Fair	Poor	Poor
Tube alignment	Very high	Very high	High	High	High
Tube type	Hollow	Hollow	Bamboo	Bamboo	Bamboo

Deposition conditions: CH_4/H_2 = 15 sccm:15 sccm; microwave power, 800 W; bias, −200 V; and magnetic field, 875 G.

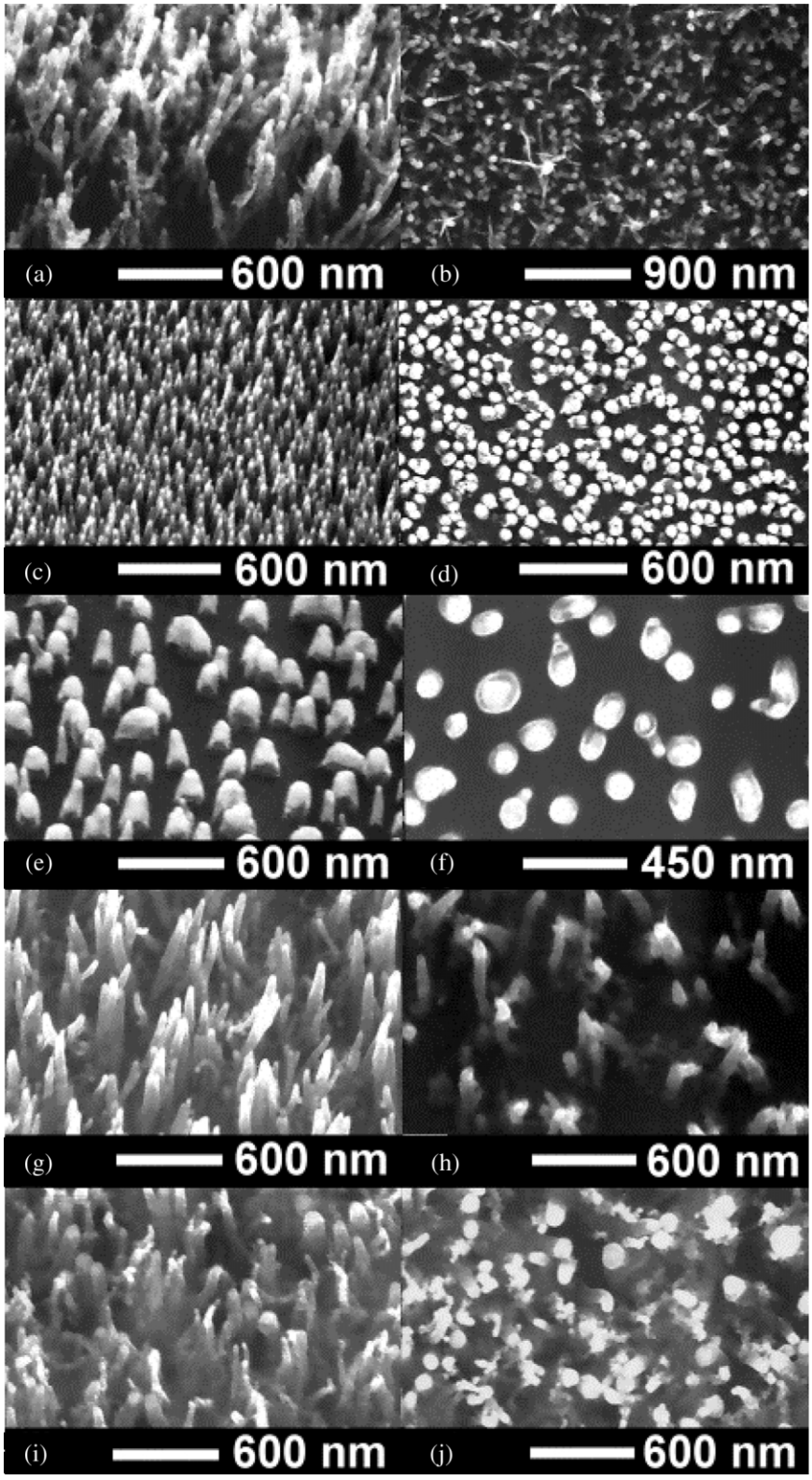

Fig. 1. SEM micrographs of the different catalyst-assisted CNTs: (a) Fe, side view; (b) Fe, top view (specimen D1); (c) Fe–Pt, side view; (d) Fe–Pt, top view (specimen A1); (e) Co–Pt, side view; (f) Co–Pt, top view (specimen B1); (g) $Nd_2Fe_{14}B$, side view; (h) $Nd_2Fe_{14}B$, top view (specimen C1); (i) Fe–Ni, side view; and (j) Fe–Ni, top view (specimen E1).

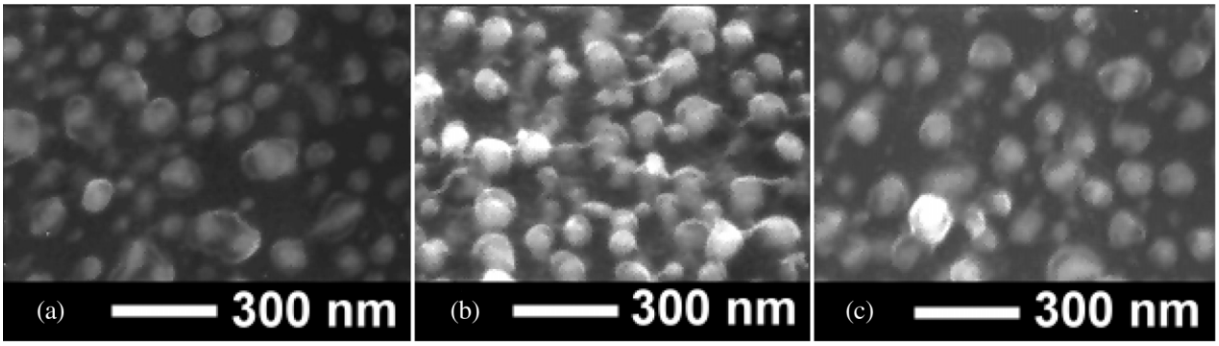

Fig. 2. SEM micrographs of the different catalyst-encapsulated carbon nano-particles without the catalyst H plasma pretreatment: (a) Fe (specimen D2); (b) Fe–Pt (specimen A2); and (c) Co–Pt (specimen B2).

CNTs. These differences in structure or properties may relate to the solubility difference of carbon in catalysts, interaction of the catalyst with the substrate, and the etching rate difference between CNTs and carbon films in hydrogen plasma. For example, the carbon solubility of Fe is much better than Fe–Pt, and Co is much better than Co–Pt, due to the very limited carbon solubility of non-ferrous metals, such as Pt. Under the present conditions, the maximum tube number density reached 134 Gtubes/inch^2 for Fe-assisted CNTs. The tube number density is one of the main factors determining the media recording density. The longest tube length can reach 2100 nm for 15 min of deposition time for $Nd_2Fe_{14}B$-assisted CNTs, which approximately corresponds to the highest growth rate. The highest coercive force is $\sim$750 Oe for the Fe-assisted CNTs. It is interesting to note that bamboo-like CNTs can be formed without using nitrogen gas, although nitrogen was proposed as one of the main parameters for the formation of bamboo-like CNTs [10,11]. For certain applications, if the removal of catalysts from the tips of CNTs is required, this can easily be achieved by selecting a suitable catalyst combined with ultrasonic agitation in an acetone bath, e.g. Fe–Pt and Co–Pt catalysts.

3.2. Effects of hydrogen plasma pretreatment

SEM micrographs for the magnetic metal-assisted CNTs or nanoparticles show differences in the catalysts with and without hydrogen plasma pretreatments by comparing Fig. 1a with Fig. 2a, Fig. 1c with Fig. 2b, and Fig. 1e with Fig. 2c for Fe, Fe–Pt and Co–Pt catalysts, respectively. It is obvious that the morphology of the carbon nanostructures changes from tube-like to particle-like shapes on omitting the hydrogen plasma pretreatment step. From the point of view of applications in recording media, the particle-like shapes have the advantage of being short and rigid.

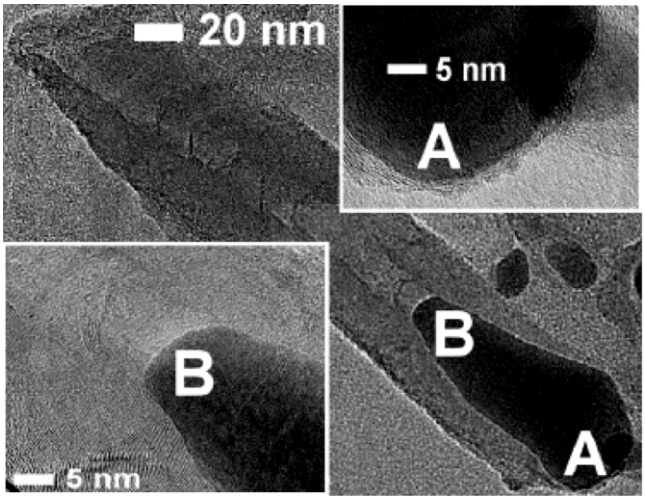

Fig. 3. Lattice image of the $Nd_2Fe_{14}B$-assisted CNTs close to the catalyst particle area (specimen C1).

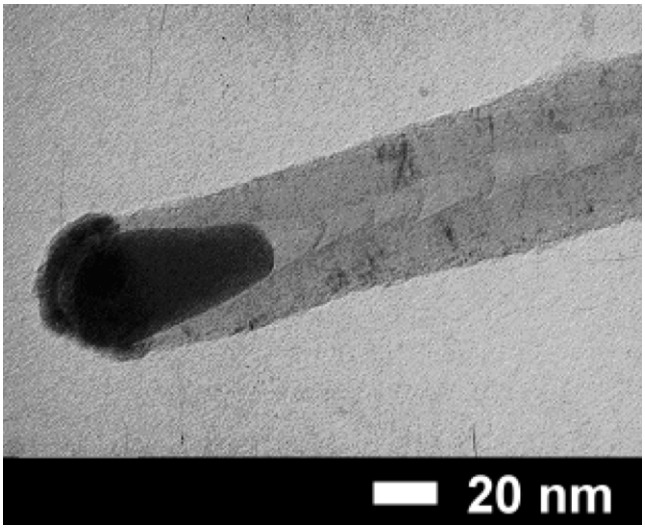

Fig. 4. HRTEM image of the Fe-assisted CNTs close to the catalyst particle area (specimen D1).

Table 3
The magnetic properties and structure features of the magnetic catalyst-assisted CNTs

Specimen designation	Catalyst material	Diameter of catalyst particle (nm)	Tube number density (Gtubes/inch^2)	$H_{c,V}$ (Oe)	$H_{c,H}$ (Oe)
A1	Fe–Pt	40	77	–	–
B1	Co–Pt	20–120	16	–	–
C1	$Nd_2Fe_{14}B$	35	71	705	350
D1	Fe	35	134	750	450
E1	Fe–Ni	10–100	39	300	300

$H_{c,V}$, coercive force in the vertical direction of the substrate surface; $H_{c,H}$, coercive force in the horizontal direction of the substrate surface.

3.3. Catalyst shape

Typical TEM and HRTEM lattice images of the $Nd_2Fe_{14}B$- and Fe-assisted CNTs close to the catalyst particles are shown in Figs. 3 and 4, respectively. In addition to the advantage of the vertically aligned CNTs, the catalysts at the tips of the CNTs are pear-like in shape, which favor a greater contribution from magnetic shape anisotropy. The present process under ECR conditions with magnetic field strength of 875 G may also take the advantage of a magnetic annealing effect to enhance the induced anisotropy. The magnetic properties and structure features of the magnetic catalyst-assisted CNTs are shown in Table 3. The catalyst particles show a wider size distribution, from 10 to 120 nm in diameter, for the Co–Pt and Fe–Ni catalysts. In contrast, the catalyst particles are more uniform in size, approximately 35–40 nm in diameter, for the Fe, $Nb_2Fe_{14}B$ and Fe–Pt catalysts. It seems that the uniform particle size results in greater coercive force and magnetic anisotropy. This may relate to a size greater than but close to the critical optimum size or single domain size, which favors higher coercive force [11,12]. The greatest coercive force can reach 750 Oe for Fe-assisted CNTs at a deposition temperature of 715 °C, which is comparable with values reported in the literature. The difference in coercive force between the vertical and horizontal directions can reach 300 Oe for Fe-assisted CNTs, and 355 Oe for $Nb_2Fe_{14}B$-assisted CNTs.

3.4. Effect of deposition temperature

The two typical hysteresis loops of the $Nd_2Fe_{14}B$-assisted CNTs in the vertical and horizontal directions of the substrate surface are shown in Fig. 5. The coercive force of the $Nd_2Fe_{14}B$-assisted CNTs as a function of deposition temperature is shown in Fig. 6. It is obvious that the higher deposition temperature favors greater coercive force and greater anisotropy. The abnormally high anisotropy at temperatures greater than 700 °C is not understood. It may relate to temperatures high enough to enhance the magnetic annealing effect. At high enough temperatures, the aspect ratio of the catalyst particle may also be increased during CNT growth by reducing the viscosity of the catalyst.

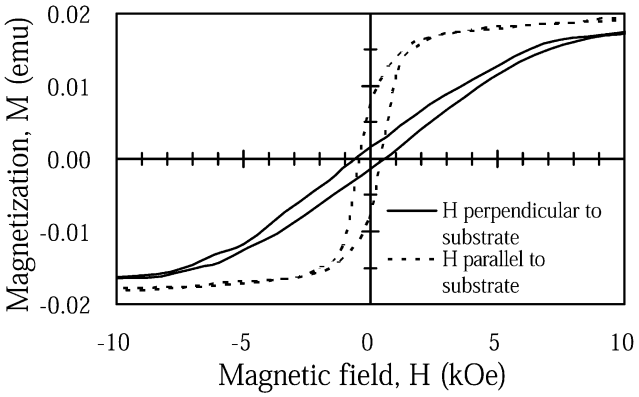

Fig. 5. Two typical hysteresis loops of the $Nd_2Fe_{14}B$-assisted CNTs in both vertical and horizontal directions to the substrate surface (specimen C6).

3.5. AFM and MFM images

The AFM and the corresponding MFM images and MFM line-scan profiles for the Fe-, Fe–Pt- and Co–Pt-assisted nanoparticles or CNTs are shown in Fig. 7a–c, d–f and g–i, respectively. The brighter and darker areas in the MFM images represent areas with repulsive and attractive magnetic forces to the MFM probe, respectively. This implies that the magnetic particles are well distributed, and the magnetic field of each particle can be detected or read.

4. Conclusions

Five different magnetic materials were successfully used to act as catalysts for the synthesis of magnetic

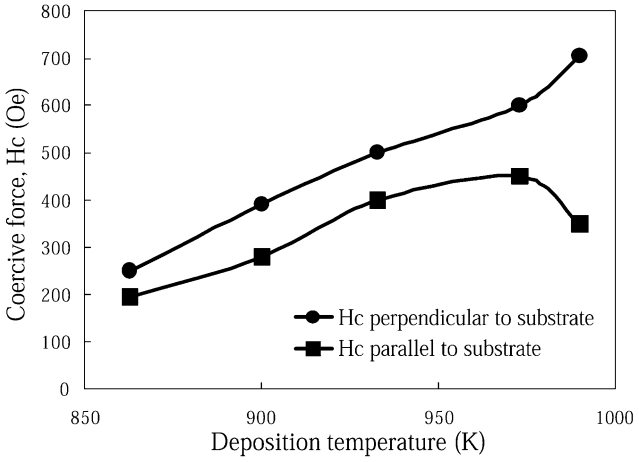

Fig. 6. Coercive forces in the vertical and horizontal directions vs. deposition temperature for the $Nd_2Fe_{14}B$-assisted CNTs (specimens C1–C6).

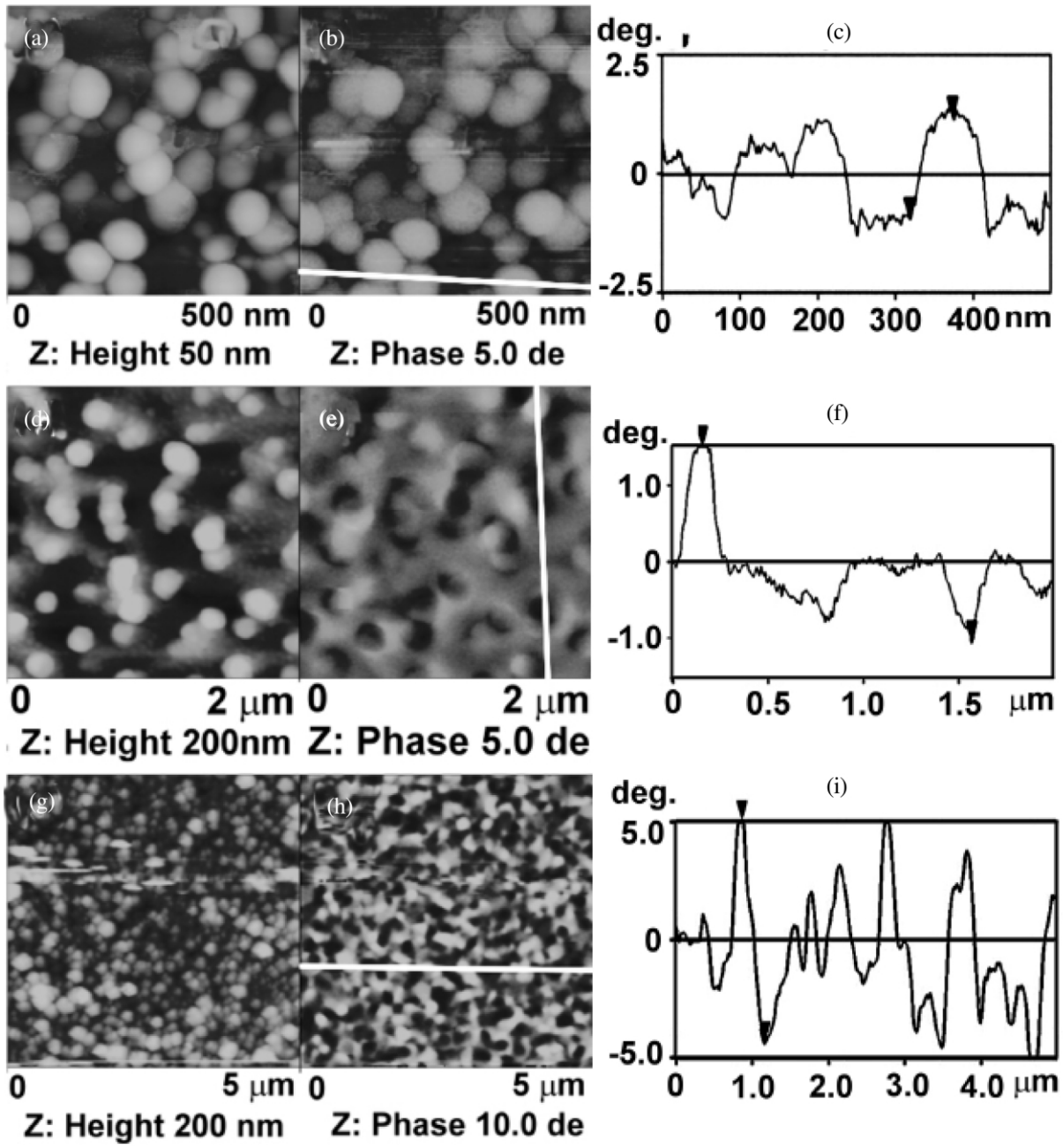

Fig. 7. AFM image, MFM image and the corresponding MFM line scan profile for different catalyst-assisted CNTs or nano-particles, respectively: (a,b,c) Fe (specimen D2); (d,e,f) Fe–Pt (specimen A1); (g,h,i) Co–Pt (specimen B2).

metal-encapsulated CNTs or nanoparticles on Si wafer to study their feasibility for perpendicular recording-media applications. The results show that we can successfully deposit perpendicularly-aligned magnetic particle-embedded nanotubes and nanoparticles. For recording media applications, most of the deposited CNTs take advantage of tip-growth and perpendicularly aligned CNTs. CNTs with different tube number density, tube length, carbon film formation, bonding between catalyst and CNTs, growth mechanism and type of CNT can be manipulated by selecting different catalysts and pretreatments. These differences in structure or properties may relate to the different solubility of carbon in the catalysts, interaction of the catalyst with the substrate and the etching rate difference between CNTs and carbon films in hydrogen plasma. The tube number density is a key parameter determining the density of the recording media. Under the present conditions, the maximum tube number density can reach 134 Gtubes/inch^2 for Fe-assisted CNTs.

With regard to the magnetic properties of the magnetic metal-encapsulated carbon nanostructures, the grain size of the magnetic particles (35–40 nm in diameter) is greater than but close to the critical optimum size or single domain size, which favors a higher coercive force. A higher CNT deposition temperature results in a greater coercive force due to smaller catalyst size; the greatest coercive force can reach 750 Oe for Fe-assisted CNTs at a deposition temperature of 715 °C, which is comparable to values reported in the literature [12–15]. The process also takes advantages of higher shape and induced anisotropy due to its higher aspect ratio and magnetic annealing effect. The coercive force difference between the vertical and horizontal directions can reach 355 Oe under the present conditions. The results also demonstrate the potential applications in magnetic recording media of the isolated and well-distributed magnetic particles in the magnetic metal-encapsulated carbon nanostructures as imaged by MFM micrographs.

Acknowledgments

This work was supported by the National Science Council (Contract No NSC90-2216-E-009-040, -034 and -035) of Taiwan.

References

[1] M. Todorovic, S. Schultz, J. Wong, A. Scherer, Appl. Phys. Lett. 74 (1999) 2516.
[2] D.E. Speliotis, J. Magn. Magn. Mater. 193 (1999) 29.
[3] S.Y. Chou, Proc. IEEE 85 (1997) 652.
[4] S.Y. Chou, P.R. Krauss, J. Magn. Magn. Mater. 155 (1996) 151.
[5] S.Y. Chou, P.R. Krauss, L. Kong, J. Appl. Phys. 79 (8) (1996) 6101.
[6] S. Iwasaki, K. Takemura, IEEE Trans. Magn. 11 (5) (1975) 1173.
[7] S. Iwasaki, Y. Nakamura, IEEE Trans. Magn. 13 (5) (1977) 1272.
[8] R.L. White, J. Magn. Magn. Mater. 209 (2000) 1.
[9] D.L. Leslie-Pelecky, R.D. Rieke, Chem. Mater. 8 (1996) 1770.
[10] X. Ma, E. Wang, D.A. Jefferson, et al., Appl. Phys. Lett. 75 (1999) 3105.
[11] H.L. Chang, C.H. Lin, C.T. Kuo, Diamond Relat. Mater. 11 (3–6) (2002) 793.
[12] X.X. Zhang, G.H. Wen, S. Huang, L. Dai, R. Gao, Z.L. Wang, J. Magn. Magn. Mater. 231 (2001) L9.
[13] N. Grobert, W.K. Hsu, Y.Q. Zhu, et al., Appl. Phys. Lett. 75 (1999) 3363.
[14] X. Sun, G.A. Yacaman, M. Jose, D. Xinglong, J. Shouri, Mater. Sci. Eng. A 286 (2000) 157.
[15] T. Hayashi, S. Hirono, M. Tomita, S. Umemura, Nature 381 (1996) 772.